Shock Waves (2005) 14(5/6): 421–424
DOI 10.1007/s00193-005-0281-6

TECHNICAL NOTE

V. Menezes · S. Kumar · K. Maruta · K.P.J. Reddy · K. Takayama

Hypersonic flow over a multi-step afterbody

Received: 27 June 2005 / Accepted: 4 October 2005 / Published online: 22 November 2005

Abstract Effect of a multi-step base on the total drag of a missile shaped body was studied in a shock tunnel at a hypersonic Mach number of 5.75. Total drag over the body was measured using a single component accelerometer force balance. Experimental results indicated a reduction of 8% in total drag over the body with a multi-step base in comparison with the base-line (model with a flat base) configuration.The flow fields around the above bodies were simulated using a 2-D axisymmetric Navier–Stokes solver and the simulated results on total drag were compared with the measured results. The simulated flow field pictures give an insight into the involved flow physics.

Keywords Drag measurement · Stepped afterbody · Accelerometer balance · Hypersonic

PACS 47.40.Ki

1 Introduction

The topic of drag reduction has been and continues to be an issue of considerable interest in view of improving the aerodynamic efficiency of flight vehicles. The base drag, arising out of flow separation behind blunt bases can be significant in the cases of missiles, projectiles, and other aircraft afterbodies. Many researchers have pursued the study of base flow drag reduction over a long period of time, but most of these studies are pertinent to transonic and supersonic flows [1–3]. But the problem of wake flow at hypersonic speeds and the drag associated with it could also be a significant source of observation in the design of vehicles. The current paper presents a very brief study concerning the drag measurements on a missile-shaped body with and without the addition of a multi-step afterbody. Of interest here is the evaluation of this drag reduction device at a hypersonic Mach number of 5.75 in a shock tunnel. It is believed that the multi-step afterbodies permit the use of shorter and possibly lower cost afterbodies in comparison with the customary boat-tailed or conical afterbodies [1].

Communicated by K. Takayama

V. Menezes (✉) · K. Takayama
Interdisciplinary Shock Wave Research Center, TUBERO,
Tohoku University, Sendai 980-8577, Japan
E-mail: viren@rainbow.ifs.tohoku.ac.jp

S. Kumar · K. Maruta
Institute of Fluid Science, Tohoku University, Sendai 980-8577, Japan

K. P. J. Reddy
Department of Aerospace Engineering, Indian Institute of Science,
Bangalore 560-012, India

2 Experiments

The experiments were carried out in a hypersonic shock tunnel [HST2] at a free stream Mach number of 5.75 [4]. Typical free stream conditions for the experiments are given in Table 1. Flow total enthalpy and the effective test time for these experiments were 1.2 MJ/kg and 800 μs, respectively. The test model had a conical leading end terminating in a hemispherical nose, as shown in Fig. 1. The middle portion of the model was a concentric cylinder to which another flat, cylindrical afterbody of 50 mm length was attached to form the base-line configuration. A five-step afterbody with uniform step heights and lengths was attached to the middle cylinder, replacing the flat, cylindrical afterbody, to form a multi-step afterbody configuration.

A single-component accelerometer balance [5] was used to measure the drag force on the body. The balance comprised a PCB-Piezotronics accelerometer and two flexible, circular rubber bushes on which the model was suspended. A cylindrical sting was passed through the centers of these flexible bushes and the model was fastened in the test section using the sting. The rubber bushes had a stiffness of 175 N/cm in bending and for a short test time of less than a millisecond, the restraint offered by these bushes was negligible, making the model totally unrestrained during the test. The accelerometer in the balance was fixed on the inner side of the model nose, along the model axis, and had a maximum sensitivity and frequency of 10 mV/g and 10 kHz,

Table 1 Typical test conditions in shock tunnel

Test gas	Air ($\gamma = 1.4$)
$h_{0\infty}$(MJ/kg)	1.2±3%
V_∞(m/s)	1400±2%
T_∞(K)	140±3%
ρ_∞(kg/m^3)	0.01±3%
M_∞	5.75
Re_∞(m^{-1})	1.4×10^6 ±1%

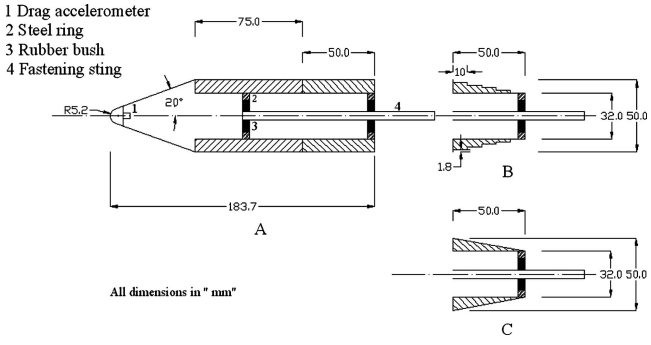

Fig. 1 Test models; **A**: base-line configuration, **B**: five-step afterbody, **C**: conical afterbody (used only for simulations)

respectively. The axial force *C(t)* on the model and the aerodynamic drag coefficient C_d were calculated from the following equations:

$$C(t) = \left[\frac{w}{g}\right]\xi \tag{1}$$

$$C_\mathrm{d} = \left[\frac{C(t)}{(q_\infty S_b)}\right] \tag{2}$$

where, w is the mass of the model, g is the acceleration due to gravity, ξ is the measured acceleration from the axial accelerometer (i.e., mean value of the signal voltage-rise in the steady state region ÷ accelerometer sensitivity), q_∞ is the free stream dynamic pressure in the tunnel test section (i.e., $\frac{\gamma}{2} p_\infty M_\infty^2$) and S_b is the reference area based on the maximum diameter on the model.

3 Numerical simulations

The flow fields over the body with different bases were simulated using a commercial CFD code *Fluent 6.1*, in order to understand the involved flow physics. Axi-symmetric Navier–Stokes equations were solved assuming appropriate boundary conditions, which were based on the experimental conditions in the shock tunnel. A typical grid used for the present simulations is shown in Fig. 2. The structured grid was generated using the *Gambit* grid generator. Grid adaptations were carried out to refine the mesh till the solution became mesh independent. The pressure and velocity gradient variables were used as the mesh refinement variables. A 2-D,

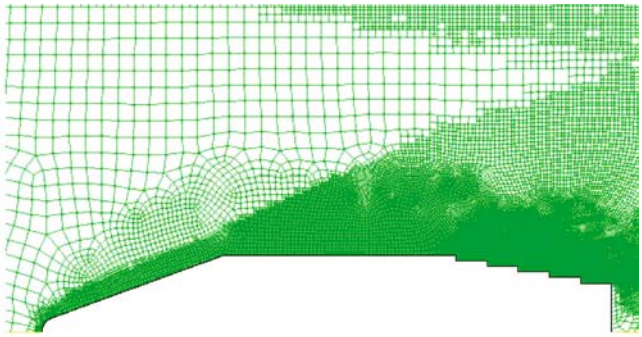

Fig. 2 Typical grid used for the simulations

axi-symmetric, coupled solver was used to solve the governing equations in the computational domain. A second-order discretization scheme was used to solve the momentum and energy equations in the flow domain. The base flow is governed by boundary layer separation and re-attachment processes that may make the flow turbulent. Hence, a standard $k - \epsilon$ turbulence model was used to simulate the turbulent flow behavior in the domain. The solution was deemed to be converged when the residuals of all the variables fell below 1×10^{-4}, while a residual of 1×10^{-6} was used for the energy equation. A conical afterbody of the same dimensions as that of the stepped base was included in the computational study to check the effectiveness of short, conical afterbodies as base drag-reducing devices.

4 Results and discussion

High-speed base flows for the flat and stepped afterbodies are schematically shown in Fig. 3. On a flat afterbody, the flow pressure on the cylindrical surface does not oppose the drag on the body, and in the wake of this afterbody, the pressure drops due to a massive expansion and separation of the flow. Hence, the drag on the body in this case has a very low opposing force. In the case of a stepped afterbody, if the step height is kept approximately equal to the boundary layer thickness ahead (upstream) of it, then the separated flow at each step would re-attach at the horizontal face of the step before passing onto the next step downstream, giving rise to

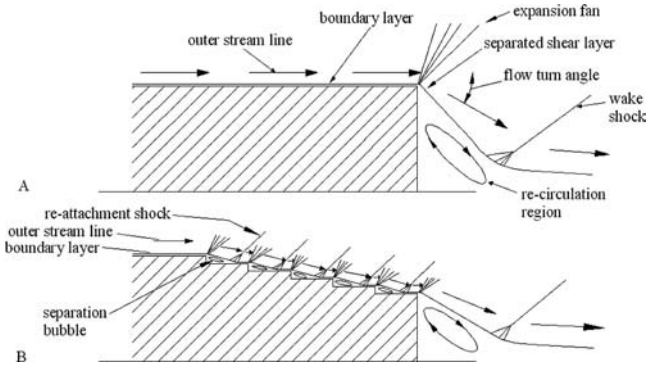

Fig. 3 Schematic of base flow; **A**: flat base, **B**: base with steps

Table 2 Drag coefficient (C_d) for the model with different afterbodies

Model configuration	C_d measured	C_d computed
Base-line	$0.37 \pm 2.3\%$	0.379
Base with five steps	$0.34^{+3\%}_{-2\%}$	0.345
Conical base	–	0.364

a controlled flow separation thereby generating a weak separation bubble at the step [3]. This trapped separation bubble between the vertical wall of the step and the re-attachment point is steady, unless there is a feedback of the flow from the re-attachment point. The subsequent flow separation and re-attachment at every step ensures that the external flow over the afterbody follows the steps fairly closely, with a good pressure recovery; and moreover, the flow expansion in the wake is gradual when compared to the flat base. The external (effective) flow turn angle over the steps is much smaller in comparison with the one in the wake of the flat base, and hence, the flow pressure is higher on the steps when compared to the pressure in the wake of the flat base. The pressure on the steps is also exerted on the vertical surfaces of the steps, which opposes the axial force on the body. Moreover, the flow separation reduces skin friction on each step, thereby reducing viscous drag on the afterbody. Due to these flow characteristics, the drag on a stepped afterbody is lower when compared to its flat counterpart. In the present case, the first step height for the afterbody was chosen on par with the boundary layer thickness ahead of it, which was around 1.8 mm. This value of boundary layer thickness was based on the simulated flow field pictures.

Table 2 gives the experimental and computed values of coefficient of drag (C_d) for the body with different afterbodies. As indicated in the table, the bodies with modified bases have lower values of C_d in comparison with that for the flat base, and the numerical results indicate that the model with the stepped afterbody has the lowest value of C_d. The model acceleration signals obtained from the accelerometer balance during the tests in the shock tunnel, for identical test conditions, are presented in Fig. 4. The level of acceleration for both the models looks almost the same in the figure, but since the models have different masses, the value of drag force works out to be different for each model. Table 3 gives the percentage of drag reduction on the model with the modified bases. The model with the stepped afterbody gives approximately 8–9% reduction in total drag when compared to the base-line configuration, and the numerical results predict about 4% reduction in total drag for the model with the conical afterbody. Though the conical afterbody offers a considerable pressure recovery, the viscous drag generated in this case is much higher when compared to the stepped base.

Table 3 Reduction in drag for the model with modified bases

Model configuration	Drag reduction measured	Drag reduction computed
Base with five steps	8.1%	8.97%
Conical base	–	3.96%

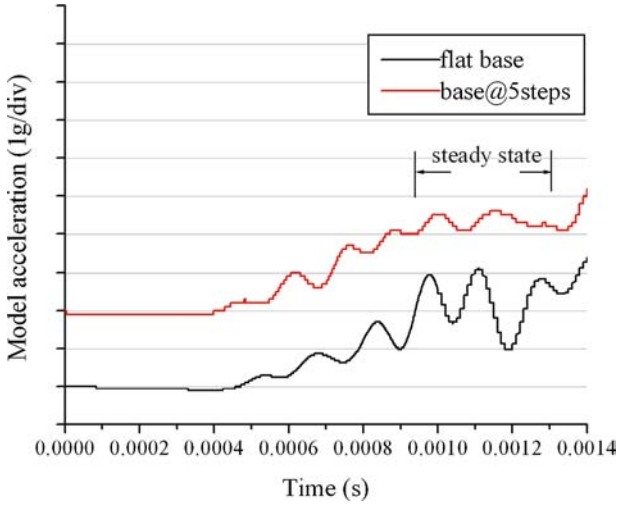

Fig. 4 Model acceleration signals from the balance during a test in the shock tunnel

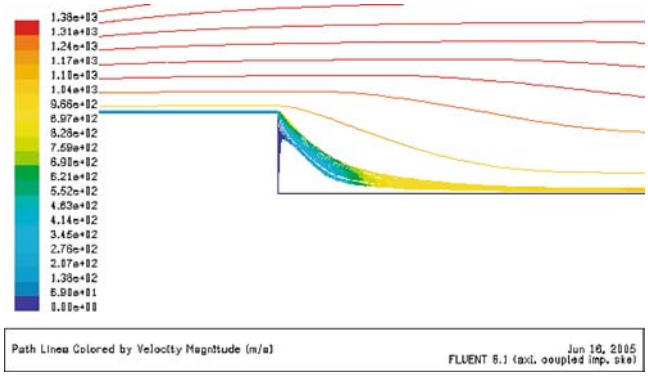

Fig. 5 Simulated path lines of velocity (m/s) over the flat base

Figures 5–8 show the simulated velocity path lines over different bases. The flow in the wake of the flat base undergoes a massive expansion with a large flow turn angle as seen in Fig. 5. Having a stepped afterbody with appropriate step height and length would make the flow turn smoothly and also fairly closely to the steps, as shown in Fig. 6, with a good pressure recovery, such that the pressure force on the vertical walls of the steps opposes the drag on the body. The separated shear layer gets re-attached at every step of this afterbody, as shown in Fig. 7, and in the wake, the flow expansion is gradual when compared to the flat base. On every step of the afterbody, a separation bubble covers a substantial portion of the horizontal surface area, which in turn reduces the wetted area thereby reducing the skin friction drag. The flow turn angle over the conical afterbody, as seen in Fig. 8, is quite similar to the one over the stepped afterbody, but the drag on the conical afterbody is larger due to the increased wetted area, which presumably increases the skin friction drag.

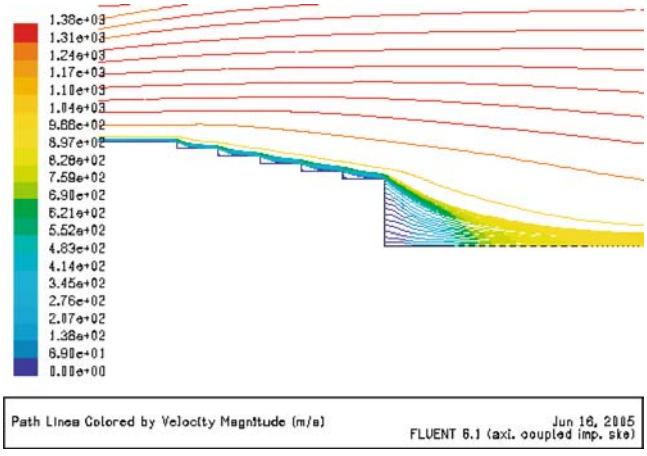

Fig. 6 Simulated path lines of velocity (m/s) over the multi-step afterbody

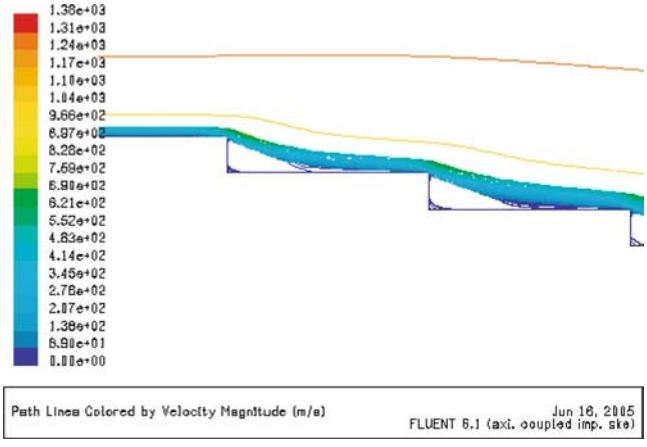

Fig. 7 Simulated path lines of velocity (m/s) over the multi-step afterbody

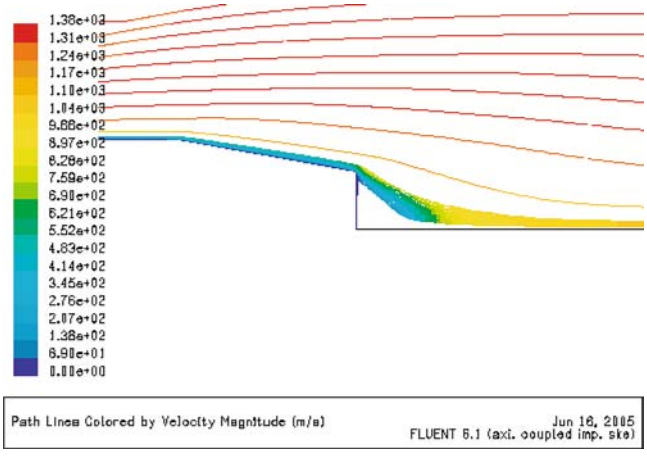

Fig. 8 Simulated path lines of velocity (m/s) over the conical base

5 Conclusion

Drag measurements were carried out on a missile-shaped model, with and without modified bases, using an accelerometer balance in a shock tunnel at Mach 5.75. Preliminary experimental results indicated about 8 % reduction in total drag for the model with a multi-step afterbody. Numerical simulations were carried out on the model with two afterbodies; a multi-step afterbody and a conical afterbody. Axisymmetric N-S solutions with a standard $k - \epsilon$ turbulence model showed very similar results on the coefficient of drag values for the body, and the simulated flow field pictures give an insight into the involved flow physics. The experimental results also serve to validate the CFD codes for such high-speed, turbulent flows. Further investigations are planned with bodies with different step configurations at hypersonic speeds.

References

1. Kentfield, J.A.C.: Short, multi-step, afterbody fairings. J. Aircraft **21**, 351–352 (1984)
2. Tanner, M.: Base pressure in supersonic flow: Further thoughts about a theory. AIAA J. **30**, 565–567 (1991)
3. Viswanath, P.R.: Drag reduction of afterbodies by controlled separated flows. AIAA J. **39**, 73–78 (2001)
4. Menezes, V., Saravanan, S., Reddy, K.P.J.: Shock tunnel study of spiked aerodynamic bodies flying at hypersonic Mach numbers. Shock Waves **12**, 197–204 (2002)
5. Menezes, V., Saravanan, S., Jagadeesh, G., Reddy, K.P.J.: Experimental investigations of hypersonic flow over highly blunted cones with aerospikes. AIAA J. **41**, 1955–1966 (2003)